HHS Public Access

Author manuscript

Cell Rep. Author manuscript; available in PMC 2016 May 05.

Published in final edited form as:

Cell Rep. 2016 May 3; 15(5): 978–987. doi:10.1016/j.celrep.2016.03.085.

KRAS-MEK Signaling Controls Ago2 Sorting into Exosomes

Andrew J. McKenzie[1,8], **Daisuke Hoshino**[2], **Nan Hyung Hong**[1], **Diana J. Cha**[3], **Jeffrey L. Franklin**[4,5,6], **Robert J. Coffey**[4,5,6], **James G. Patton**[3], and **Alissa M. Weaver**[1,5,7,*]

[1]Department of Cancer Biology, Vanderbilt University School of Medicine, Nashville, TN 37232, USA

[2]Division of Cancer Cell Research, Kanagawa Cancer Center, Yokohama 241-8515, Japan

[3]Department of Biological Sciences, Vanderbilt University, Nashville, TN 37232, USA

[4]Department of Medicine, Vanderbilt University Medical Center, Nashville, TN 37232, USA

[5]Department of Cell and Developmental Biology, Vanderbilt University School of Medicine, Nashville, TN 37232, USA

[6]Veterans Affairs Medical Center, Nashville, TN 37232, USA

[7]Department of Pathology, Microbiology and Immunology, Vanderbilt University Medical Center, Nashville, TN 37232, USA

Summary

Secretion of RNAs in extracellular vesicles is a newly recognized form of intercellular communication. A potential regulatory protein for microRNA (miRNA) secretion is the critical RNA-induced silencing complex (RISC) component Argonaute 2 (Ago2). Here, we use isogenic colon cancer cell lines to show that overactivity of KRAS due to mutation inhibits localization of Ago2 to multivesicular endosomes (MVEs) and decreases Ago2 secretion in exosomes. Mechanistically, inhibition of mitogen-activated protein kinase kinases (MEKs) I and II, but not Akt, reverses the effect of the activating KRAS mutation and leads to increased Ago2-MVE association and increased exosomal secretion of Ago2. Analysis of cells expressing mutant Ago2 constructs revealed that phosphorylation of Ago2 on serine 387 prevents Ago2-MVE interactions and reduces Ago2 secretion into exosomes. Furthermore, regulation of Ago2 exosomal sorting controls the levels of three candidate miRNAs in exosomes. These data identify a key regulatory signaling event that controls Ago2 secretion in exosomes.

Graphical abstract

*Correspondence: alissa.weaver@vanderbilt.edu.

[8]Present address: Sarah Cannon Research Institute, Nashville, TN 37203, USA

Supplemental Information: Supplemental Information includes Supplemental Experimental Procedures, three figures, one table, and two appendices and can be found with this article online at http://dx.doi.org/10.1016/j.celrep.2016.03.085.

Author Contributions: D.H. and A.M.W. conceived of the project. A.J.M. and D.H. performed immunofluorescence microscopy, exosome purification, and analysis. A.J.M. performed subcellular fractionation and most data analysis. N.H.H. performed experiments with purified exosomes. D.J.C. performed miRNA analysis experiments. A.M.W., J.G.P., J.L.F., and R.J.C. contributed to experimental and project design. J.L.F. and R.J.C. also contributed reagents. The manuscript was written by A.J.M. and A.M.W., with contributions from all authors.

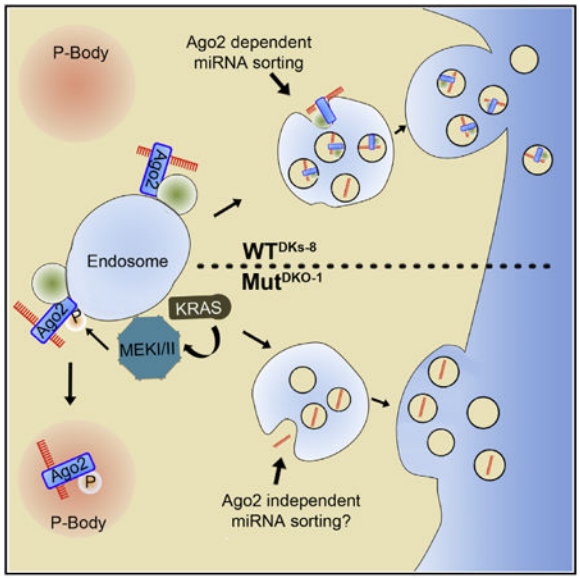

Introduction

Secretion of RNAs into the extracellular space is reported to regulate cell physiology (Patton et al., 2015). Extracellular RNAs are carried by RNA-binding proteins, lipoproteins, or extracellular vesicles (EVs) (Arroyo et al., 2011; Turchinovich et al., 2011; Valadi et al., 2007; Vickers et al., 2011). MicroRNAs (miRNAs) are a prominent component of secreted RNAs (Patton et al., 2015; Skog et al., 2008; Valadi et al., 2007). Certain miRNAs are preferentially sorted into EVs, including late-endosome-derived exosomes and shed microvesicles (MVs) (Patton et al., 2015). Exosomal miRNAs can affect recipient-cell phenotypes, including gene expression, cancer invasiveness, proliferation, and inflammatory responses (Patton et al., 2015).

Mechanistically, it is unclear how miRNAs and miRNA-associated proteins are sorted into exosomes. Some targeting sequences depend on binding to sumoylated hnRNPA2B1 (Villarroya-Beltri et al., 2013). In addition, 3′-uridylated miRNAs are preferentially sorted to exosomes in B cells (Koppers-Lalic et al., 2014). However, in most cases, these targeting sequences are not present in secreted miRNAs (Cha et al., 2015). The association of the RNA-induced silencing complex (RISC) machinery with multivesicular endosomes (MVEs) (Gibbings et al., 2009) suggests another mechanism that could control secretion of miRNAs and miRNA-mRNA complexes via exosomes.

Argonaute (Ago) 2 is a key component of the RISC that can directly degrade mRNA by slicing (Meister, 2013). Ago2 accumulates in cytoplasmic processing bodies (P-bodies), where additional binding interactions promote translational inhibition and mRNA decay (Meister, 2013; Sen and Blau, 2005). Ago2 also associates with MVEs in structures that have been termed “GW-bodies” due to the presence of GW182 but lack of other P-body components (Gibbings et al., 2009). Recent reports have demonstrated that Ago2 binds to miRNAs to generate Ago2-miRNA complexes that are found in the extracellular space. Although the majority of reports describe Ago2 as being present in the extracellular space as

a free protein (Arroyo et al., 2011; Russo et al., 2012; Turchinovich et al., 2011), other reports have shown that Ago2 and other RNA-processing proteins are contained in secreted exosomes (Melo et al., 2014; Squadrito et al., 2014).

Here, we demonstrate that KRAS-dependent activation of MEK-ERK (mitogen-activated protein kinase kinase/extracel-lular-signal-regulated kinase) signaling inhibits sorting of Ago2 and Ago2-dependent miRNAs into exosomes. These data establish a molecular mechanism for regulation of Ago2 sorting and miRNA loading into exosomes.

Results

KRAS Regulates Ago2 Localization to MVEs

We recently demonstrated that the loading of specific protein and miRNA cargos into exosomes is dependent on *KRAS* mutational status (Cha et al., 2015; Demory Beckler et al., 2013). As a class, RNA-binding proteins are greatly decreased in mutant *KRAS*-cell-derived exosomes (Demory Beckler et al., 2013). To determine whether KRAS activity affects RISC machinery association with MVEs, we performed confocal immunofluorescence microscopy on wild-type and mutant KRAS-expressing colon cancer cells (WT^{DKs-8} and Mut^{DKO-1}, respectively) (Figure 1A). WT^{DKs-8} and Mut^{DKO-1} cells were derived from DLD1 cells, which are heterozygous for the *G13D KRAS* mutation, by homologous recombination to remove mutant or WT *KRAS* genes (Shirasawa et al., 1993). Colocalization of Ago2 with the MVE marker CD63 and P-body component DCP1a revealed a large increase in Ago2-CD63 colocalization in WT^{DKs-8} compared to Mut^{DKO-1} cells (Figure 1B). Conversely, Ago2 colocalization with DCP1a was decreased in WT^{DKs-8} cells (Figure 1C). Colocalization of DCP1a with CD63 was rarely observed (Figure 1D), consistent with Gibbings et al. (2009). DCP1a-positive foci usually colocalized with Ago2; however, not all Ago2-positive foci were DCP1a positive (Figure 1E). Similar results were observed in another isogenic colorectal cancer cell line model of KRAS mutation (Figure S1A). Colocalization of Dicer or GW182 with CD63 revealed that there was a 3-fold increase in GW182-CD63 colocalization in WT^{DKs-8} cells but no effect of KRAS on Dicer-CD63 colocalization (Figures 1F–1I).

To corroborate our imaging results, we performed sub-cellular fractionation of post-nuclear extracts (PNEs) on a density gradient to separate P-bodies and MVEs (Figure 1J), as described previously (Squadrito et al., 2014). P-body components DCP1a and GW182 sedimented in less dense fractions (1–6), compared to late-endosomal MVE markers Rab7 and flotillin (fractions 7–9). Western blot analysis revealed that Ago2 cofractionates with P-body markers, regardless of KRAS status. However, significantly more Ago2 was present in MVE fractions from WT^{DKs-8} cells compared to Mut^{DKO-1} cells (Figure 1J). Quantitation of the percentage of Ago2 and Rab7 in each fraction revealed that the percentage of Ago2 cofractionating with MVE was increased by ∼3-fold in WT^{DKs-8} cells (Figures 1K and 1L). Together, the biochemical and imaging data demonstrate that mutant KRAS decreases Ago2-MVE association.

KRAS Regulates Ago2 Secretion in Exosomes

To test whether KRAS-regulated association of Ago2 and GW182 with MVE affects their secretion into EVs, conditioned media from WT^{DKs-8} and Mut^{DKO-1} cells were subjected to differential centrifugation (Théry et al., 2006). The low-speed pellet (10,000 × *g*), which typically contains shed MVs, and the highspeed pellet (100,000 × *g* for 18 hr) containing ultracentrifuged exosomes (UC exosomes) were collected. In some cases, the UC exosomes were further sedimented in a density gradient (5%–40% iodixanol) for 18 hr at 100,000 × *g,* leading to equilibration according to vesicle density (DG exosomes [DG-exo]). NanoSight analysis and transmission electron microscopy revealed typical size profiles for exosomes and MVs that was similar in both cell lines (Figures S1B and S1C); however, Mut^{DKO-1} cells secreted more UC exosomes compared to WT^{DKs-8} cells (Figure S1D)

Comparison of equal numbers of UC exosomes by western blot analysis revealed a decrease in Ago2 and GW182 in Mut^{DKO-1} exosomes compared to WT^{DKs-8} exosomes (Figures 1M and 1N), despite equivalent whole-cell Ago2 levels (Figures 1O and 1P). Similarly, UC exosomes isolated from $Mut^{HCT-116}$ had decreased Ago2 levels, compared to exosomes isolated from the isogenic cell line WT^{HKe-3} (Figure S1E). There was no significant difference in Dicer levels between WT^{DKs-8} and Mut^{DKO-1} exosomes (Figures 1M and 1N). The P-body protein, DCP1a, was undetectable in exosomes (data not shown), consistent with its lack of colocalization with MVEs (Figures 1A and 1D) (Gibbings et al., 2009). Ago2 levels were similar, and Dicer and GW182 were undetectable in MVs purified from WT^{DKs-8} and Mut^{DKO-1} cells (Figures 1M and 1N). These data are consistent with regulation of RISC association with MVEs by KRAS.

Since UC exosomes may contain non-vesicle-associated protein aggregates, and Ago2 can be present in bodily fluids as a non-vesicular protein complex (Arroyo et al., 2011; Turchinovich et al., 2011), we further purified UC exosomes by density gradient (DG-exo; Figure 1Q). Analysis of WT^{DKs-8} DG-exo revealed that Ago2 and exosomal markers cofractionate at the expected exosome density (Figure 1Q). Very little Ago2 was detected in denser fractions corresponding to protein aggregates (Sung et al., 2015) or lighter fractions corresponding to soluble proteins (Van Deun et al., 2014). Western blot comparison of equal numbers of WT^{DKs-8} and Mut^{DKO-1} DG-exo revealed ∼4-fold less Ago2 in Mut^{DKO-1} exosomes (Figures 1R and 1S). To further demonstrate Ago2 association with exosomes, WT^{DKs-8} DG-exo were immunoprecipitated using an anti-CD63 antibody. The majority of Ago2 was coprecipitated and depleted from the supernatant by the anti-CD63 antibody but not the immunoglobulin G (IgG) control antibody (Figure S1F). Finally, to determine whether Ago2 is on the inside or outside of our purified exosomes, we used a dot-blot assay (Lai et al., 2015). WT^{DKs-8} exosomes were spotted onto nitrocellulose and probed with anti-Ago2 or anti-CD63 antibodies in the presence or absence of 0.1% Tween 20 to permeabilize the vesicles. Consistent with Ago2 being an internal exosome cargo, Ago2 was detected at much higher intensity in the presence of detergent (Figure S1G, upper panel). Consistent with its known location on the outside of exosomes, CD63 was detected in both the absence and presence of Tween 20. We found similar results using exosomes purified from cells expressing mCherry-tagged Ago2 and probed with an antibody against mCherry (Figure S1G, lower panel).

MEK Signaling Downstream of KRAS Negatively Regulates Ago2-MVE Interactions

KRAS is likely to signal through MEKI/II and downstream ERK. Alternatively, Akt and p38-MAPK (mitogen-activated protein kinase) are candidates, as they can phosphorylate Ago2 and regulate its localization to P-bodies (Horman et al., 2013; Zeng et al., 2008). To determine whether MEKI/II, Akt, or p38-MAPK regulate Ago2 localization to MVEs downstream of KRAS, Mut^{DKO-1} cells were treated for 4 hr with inhibitors to MEKI/II (PD0325901), Akt (triciribine), or p38-MAPK (SB203580). As in Figure 1, colocalization of Ago2 with CD63 was minimal in untreated Mut^{DKO-1} cells and significantly higher in WT^{DKs-8} cells (Figures 2A and 2B). However, inhibition of MEK1/2 in Mut^{DKO-1} cells increased Ago2-CD63 colocalization to levels observed in WT^{DKs-8} cells. By contrast, inhibition of Akt only partially increased Ago2-CD63 colocalization. Inhibition of p38-MAPK had no effect on Ago2-CD63 colocalization (Figures 2A and 2B). Increases in Ago2-CD63 colocalization were paralleled by concurrent decreases in Ago2-DCP1a colocalization in drug-treated Mut^{DKO-1} cells (Figure 2C). These data suggest that KRAS-MEK signaling shifts the localization of Ago2 from MVEs to P-bodies.

To corroborate these data, triciribine- or PD0325901-treated Mut^{DKO-1} cells were subjected to subcellular fractionation. As expected, MEKI/II inhibition increased the amount of Ago2 present in MVE fractions (Figures 2D–2F). Akt inhibition had a small but insignificant effect on Ago2-Rab7 cofractionation (Figure 2F), suggesting that MEK I/II and not Akt is the major signaling pathway downstream of KRAS that affects Ago2-MVE association.

KRAS-MEK Signaling Affects Ago2 Secretion into Exosomes

To determine whether MEKI/II regulates Ago2 sorting into exosomes, exosomes were collected from drug-treated cells. All cell preparations were >90% viable at the time of conditioned media collection (Figure S2A). There was no significant effect of drug treatment on exosome size; however, Akt or MEKI/II inhibition caused an ∼2-fold increase in exosome secretion (Figure S2B). To analyze cargo differences, equal numbers of exosomes were analyzed by western blotting. Inhibition of MEK I/II, but not Akt, led to Ago2 accumulation in Mut^{DKO-1} exosomes, comparable to the Ago2 levels in WT^{DKs-8} exosomes (Figures 2G and 2H). Likewise, inhibition of ERK1/2 with FR180204 increased Ago2 levels in Mut^{DKO-1} exosomes (Figures S2C and S2D). Since we collect exosomes in serum-free, growth-factor-free media, cells without mutant KRAS have minimal activation of KRAS-MEK-ERK signaling. To test whether these cells also downregulate Ago2 sorting to exosomes when KRAS-MEK-ERK signaling is activated, we collected exosomes in OptiMEM media, which is serum free but contains growth factors. Under these conditions, WT^{DKs-8} and Mut^{DKO-1} cells had equivalent activation of ERK (Figure S2E) and equivalent Ago2 levels in exosomes (Figure S2F).

Phosphorylation on S387 Inhibits Ago2 Localization to MVEs

Since phosphorylation of Ago2 at serine 387 can induce Ago2 localization to P-bodies (Horman et al., 2013; Zeng et al., 2008), we tested whether S387 phosphorylation is differentially regulated in our isogenic cells. Western blots of cell lysates from Mut^{DKO-1} and WT^{DKs-8} cells with a phosphospecific antibody revealed an ∼2-fold increase in phospho-S387 Ago2 in Mut^{DKO-1} cells. This increase was inhibited by inhibitors of Akt,

MEK I/II (Figure 3A), or ERKI/II (Figures S3A and S3B). Furthermore, pAgo2 cofractionated with P-bodies in subcellular fractionation experiments (Figure 2D). Thus, KRAS signaling drives Ago2 S387 phosphorylation through MEK, ERK, and Akt; however, only MEK/ERK signaling affects Ago2 sorting into exosomes (Figures 2G, 2H, and S2D).

To study the effect of S387 phosphorylation on Ago2-MVE interactions, mCherry-Ago2 constructs containing phosphomimetic (S387E) or phospho-resistant (S387A) mutations were expressed in Mut^{DKO-1} cells. Similar to endogenous staining of Ago2 (Figures 1 and 2), colocalization of WT- or S387E-Ago2 with CD63 was extremely low, and colocalization with DCP1a was high in Mut^{DKO-1} (Figures 3B–3D). However, colocalization of S387A-Ago2 with CD63 and DCP1a was similar to that of endogenous Ago2 in WT^{DKs-8} cells (Figures 3B–3D). Likewise, GW182-CD63 colocalization in Mut^{DKO-1} cells was increased with the expression of phospho-resistant (S387A) Ago2 (Figures S3C and S3D). These results were confirmed by subcellular fractionation (Figures 3E–3G).

Secretion of Ago2 into Exosomes Is Regulated by S387 Phosphorylation

To test whether S387 phosphorylation regulates Ago2 exosome content, conditioned media were collected from Mut^{DKO1} cells stably expressing mCherry-WT, -S387E, or -S387A Ago2 (Figure 3H). The number or size of EVs purified from these cell lines was not significantly different (Figure 3I). However, there was a 3-fold increase in S387A Ago2 found in Mut^{DKO1} exosomes compared to either WT- or S387E-Ago2 (Figures 3J and 3K). There was a similar increase in GW182 in exosomes purified from S387A-Ago2-expressing Mut^{DKO1} cells (Figures 3J and S3E). There was little effect of Ago2 phosphosite mutation on the export of Ago2 into MVs (Figures 3J and 3K).

let-7a miRNA Distribution Is Regulated by KRAS

To test whether the KRAS-dependent localization of Ago2 regulates miRNA distribution, we transfected fluorescently labeled *let-7a* (Cy3-*let-7a*) into WT^{DKs-8} and Mut^{DKO-1} cells and assessed colocalization with Ago2 and the MVE marker CD63 (Figure 4A). Regardless of KRAS status, there was ∼80% colocalization of Cy3-*let-7a* with Ago2 (Figure 4B). In WT^{DKs-8} cells, ∼90% of *let-7a*-Ago2-positive foci colocalized with CD63 (Figure 4C). However, in Mut^{DKO-1} cells, less than 10% of *let-7a*-Ago2 complexes colocalized with CD63. These data suggest that KRAS affects both Ago2 and miRNA localization.

Ago2 Affects Secretion of Candidate miRNAs into Exosomes

To test whether Ago2 regulates secretion of specific miRNAs into exosomes, we assessed the exosomal content of three candidate miRNAs in Ago2-knockdown (KD) WT^{DKs-8} cells (Figure 4D). WT^{DKs-8} cells were chosen because they secrete ∼3-fold more Ago2 into exosomes than Mut^{DKO-1} cells (Figures 1 and 2). Although the presence of Ago2 did not affect the number of secreted exosomes, there was an 8-fold decrease in the total content of small RNAs in exosomes isolated from Ago2-KD cells (Figure 4E). To determine whether there was a further selective change in *let-7a, miR-100,* and *miR-320a* levels by qRT-PCR, we adjusted the levels of RNA to 5 ng in each sample. The data revealed a significant decrease in *let-7a* and *miR-100* and no change in *miR-320a* levels in exosomes from Ago2-KD cells (Figure 4F). Analysis of the same miRNAs in total cellular RNA revealed a small

increase in *miR-320a* but no change in *let-7a* and *miR-100* levels in KD cells compared to controls (Figure 4F).

Exosomes collected from Mut^{DKO-1} cells stably expressing mCherry-WT, -S387E, or -S387A Ago2 were also analyzed for miRNA content. Compared to WT or S387A exosomes, there was a small decrease of unclear significance in the total content of small RNA in exosomes isolated from S387E Ago2 cells (Figure 4G). When examining specific miRNAs by qRT-PCR, only expression of S387A Ago2 had an effect on miRNA secretion with an ~5-fold increase in exosome levels of *let-7a, miR-100,* and *miR-320a* (Figure 4H). There was no effect of Ago2 phosphomutants on cellular expression of those miRNAs. Examination of MVs from the same cells revealed an overall lower small RNA content compared to exosomes (Figure 4G, lower panel). qRT-PCR analysis of MV RNA did not yield detectable levels of *let-7a, miR-100,* or *miR-320* in three of the four samples assayed, despite using the same amount of RNA as for exosomal RNA analyses (Table S1). Overall, these data indicate that Ago2 phosphorylation downstream of KRAS-MEK signaling controls the secretion of specific miRNAs into exosomes.

Discussion

The mechanisms by which miRNAs are sorted into EVs are not well defined. We find that Ago2 sorting into exosomes is regulated by MEK-ERK signaling downstream of activated KRAS. Phosphorylation of Ago2 on S387 specifically inhibits Ago2 association with MVEs, diminishes secretion into exosomes, and increases association with P-bodies. Both Ago2 levels and Ago2 phosphorylation control the secretion of specific miRNAs into exosomes. These data demonstrate that Ago2 can be selectively sorted into exosomes and ascribe a critical function to that event: transport of bound miRNAs for cellular secretion (see model in Figure 4I).

Whether Ago2 is present in exosomes has been controversial. In plasma, Ago2 is primarily found in non-vesicular-protein-RNA complexes (Arroyo et al., 2011; Turchinovich et al., 2011). Furthermore, only small amounts of Ago2 were found in exosomes isolated from monocytes (Gibbings et al., 2009). However, other investigators have identified Ago2 in exosomes (Melo et al., 2014). Our finding that KRAS-MEK signaling inhibits sorting of Ago2 to exosomes indicates that Ago2 is a bona fide exosome cargo; however, very low levels may be detected, due to signaling regulation. Indeed, very little Ago2 is detectable in exosomes from cells with mutant KRAS compared to Ago2 levels in exosomes purified from isogenic WT cells (Figures 1 and S1). Furthermore, growth factor stimulation of cells expressing WT KRAS is also likely to inhibit Ago2 sorting into exosomes (Figure S2) (Van Deun et al., 2014). One additional complication in interpreting the results from various studies is whether there is serum (exosome depleted or otherwise) in the collection media. Since serum contains abundant vesicle-free Ago2, it may contaminate vesicle preparations as an extravesicular-associated protein and mask intravesicular Ago2 (Van Deun et al., 2014). Since we used serum-free, growth-factor-free media, we did not have those complicating factors; thus, on density gradients, we only observed significant Ago2 in the fractions containing exosomes (Figures 1 and S1). Furthermore, our dot-blot experiments

indicate that Ago2 is primarily on the inside of vesicles in our exosome preparations (Figure S1).

Phosphorylation of Ago2 S387 previously has been shown to inhibit slicing activity, promote translational repression, and promote colocalization with P-body components (Horman et al., 2013; Zeng et al., 2008). Our study further shows that this phosphorylation event inhibits association of Ago2 with MVE and prevents secretion into exosomes. Although we confirmed that Akt activity affects phosphorylation of Ago2 S387 (Horman et al., 2013), Akt did not affect secretion of Ago2 into exosomes, whereas MEK and ERK did. We hypothesize that this difference reflects different spatial locations of signaling events. Consistent with this idea, KRAS-MEK-ERK signaling was shown to occur on late endosomes (Lu et al., 2009; Nada et al., 2009). Control of Ago2 tyrosine phosphorylation also occurs (Rüdel and Meister, 2008), and identification of the relevant kinases may suggest further spatial control. Finally, Ago2-KRAS interaction in the endoplasmic reticulum was recently shown to control KRAS levels and cellular transformation (Shankar et al., 2016), suggesting a complex interaction between KRAS and Ago2 in multiple cellular compartments.

Melo et al. (2014) found that RISC-loading complex proteins Dicer, Ago2, and TRBP were present in exosomes from breast cancer but not from normal patients. Similarly, we found Dicer and Ago2 in exosomes from colon cancer cells, along with the RISC machinery component GW182. Although Ago2 and GW182 exosome levels were regulated by KRAS, Dicer levels were not significantly changed (Figure 1). Furthermore, Ago2 phosphorylation controlled the export of GW182 into exosomes (Figures 3J and S3E). These data suggest that distinct signaling pathways may regulate sorting into exosomes of miRNA biogenesis (Dicer and TRBP) and RISC machinery molecules (Ago2 and GW182). Furthermore, our data predict that exosomes derived from tumors with KRAS mutations are likely to contain lower levels of Ago2, GW182, and miRNA than those secreted from tumors with only WT KRAS. An important future direction will be to determine whether this prediction holds in clinical samples.

In summary, our data demonstrate that oncogenic KRAS promotes the phosphorylation of Ago2 and suppresses its secretion in exosomes. We show that sorting of specific miRNAs into exosomes is controlled by Ago2. Our results implicate Ago2 as a potential major player in miRNA sorting into exosomes and identify a key regulatory signaling mechanism.

Experimental Procedures

Detailed procedures and reagent information are presented in the Supplemental Experimental Procedures.

Supplementary Material

Refer to Web version on PubMed Central for supplementary material.

Acknowledgments

Funding was provided by NIH grants U19CA179514, R01CA163563, and P50 95103 to R.J.C. Electron microscopy images were obtained through the Vanderbilt CISR, with support from NIH grants P30 CA068485, DK20593, DK58404, DK59637, and EY08126.

References

Arroyo JD, Chevillet JR, Kroh EM, Ruf IK, Pritchard CC, Gibson DF, Mitchell PS, Bennett CF, Pogosova-Agadjanyan EL, Stirewalt DL, et al. Argonaute2 complexes carry a population of circulating microRNAs independent of vesicles in human plasma. Proc Natl Acad Sci USA. 2011; 108:5003–5008. [PubMed: 21383194]

Cha DJ, Franklin JL, Dou Y, Liu Q, Higginbotham JN, Demory Beckler M, Weaver AM, Vickers K, Prasad N, Levy S, et al. KRAS-depen-dent sorting of miRNA to exosomes. eLife. 2015; 4:e07197. [PubMed: 26132860]

Demory Beckler M, Higginbotham JN, Franklin JL, Ham AJ, Halvey PJ, Imasuen IE, Whitwell C, Li M, Liebler DC, Coffey RJ. Proteomic analysis of exosomes from mutant KRAS colon cancer cells identifies intercellular transfer of mutant KRAS. Mol Cell Proteomics. 2013; 12:343–355. [PubMed: 23161513]

Gibbings DJ, Ciaudo C, Erhardt M, Voinnet O. Multivesicular bodies associate with components of miRNA effector complexes and modulate miRNA activity. Nat Cell Biol. 2009; 11:1143–1149. [PubMed: 19684575]

Horman SR, Janas MM, Litterst C, Wang B, MacRae IJ, Sever MJ, Morrissey DV, Graves P, Luo B, Umesalma S, et al. Akt-mediated phosphorylation of argonaute 2 downregulates cleavage and upregulates translational repression of MicroRNA targets. Mol Cell. 2013; 50:356–367. [PubMed: 23603119]

Koppers-Lalic D, Hackenberg M, Bijnsdorp IV, van Eijndhoven MA, Sadek P, Sie D, Zini N, Middeldorp JM, Ylstra B, de Menezes RX, et al. Nontemplated nucleotide additions distinguish the small RNA composition in cells from exosomes. Cell Rep. 2014; 8:1649–1658. [PubMed: 25242326]

Lai CP, Kim EY, Badr CE, Weissleder R, Mempel TR, Tannous BA, Breakefield XO. Visualization and tracking of tumour extracellular vesicle delivery and RNA translation using multiplexed reporters. Nat Commun. 2015; 6:7029. [PubMed: 25967391]

Lu A, Tebar F, Alvarez-Moya B, López-Alcalá C, Calvo M, Enrich C, Agell N, Nakamura T, Matsuda M, Bachs O. A clathrin-dependent pathway leads to KRas signaling on late endosomes en route to lysosomes. J Cell Biol. 2009; 184:863–879. [PubMed: 19289794]

Meister G. Argonaute proteins: functional insights and emerging roles. Nat Rev Genet. 2013; 14:447–459. [PubMed: 23732335]

Melo SA, Sugimoto H, O'Connell JT, Kato N, Villanueva A, Vidal A, Qiu L, Vitkin E, Perelman LT, Melo CA, et al. Cancer exosomes perform cell-independent microRNA biogenesis and promote tumorigenesis. Cancer Cell. 2014; 26:707–721. [PubMed: 25446899]

Nada S, Hondo A, Kasai A, Koike M, Saito K, Uchiyama Y, Okada M. The novel lipid raft adaptor p18 controls endosome dynamics by anchoring the MEK-ERK pathway to late endosomes. EMBO J. 2009; 28:477–489. [PubMed: 19177150]

Patton JG, Franklin JL, Weaver AM, Vickers K, Zhang B, Coffey RJ, Ansel KM, Blelloch R, Goga A, Huang B, et al. Biogenesis, delivery, and function of extracellular RNA. J Extracell Vesicles. 2015; 4:27494. [PubMed: 26320939]

Rüdel S, Meister G. Phosphorylation of Argonaute proteins: regulating gene regulators. Biochem J. 2008; 413:e7–e9. [PubMed: 18613814]

Russo F, Di Bella S, Nigita G, Macca V, Laganà A, Giugno R, Pulvirenti A, Ferro A. miRandola: extracellular circulating microRNAs database. PLoS ONE. 2012; 7:e47786. [PubMed: 23094086]

Sen GL, Blau HM. Argonaute 2/RISC resides in sites of mammalian mRNA decay known as cytoplasmic bodies. Nat Cell Biol. 2005; 7:633–636. [PubMed: 15908945]

Shankar S, Pitchiaya S, Malik R, Kothari V, Hosono Y, Yocum AK, Gundlapalli H, White Y, Firestone A, Cao X, et al. KRAS engages AGO2 to enhance cellular transformation. Cell Rep. 2016; 14:1448–1461. [PubMed: 26854235]

Shirasawa S, Furuse M, Yokoyama N, Sasazuki T. Altered growth of human colon cancer cell lines disrupted at activated Kiras. Science. 1993; 260:85–88. [PubMed: 8465203]

Skog J, Würdinger T, van Rijn S, Meijer DH, Gainche L, Sena-Esteves M, Curry WT Jr, Carter BS, Krichevsky AM, Breakefield XO. Glioblastoma microvesicles transport RNA and proteins that promote tumour growth and provide diagnostic biomarkers. Nat Cell Biol. 2008; 10:1470–1476. [PubMed: 19011622]

Squadrito ML, Baer C, Burdet F, Maderna C, Gilfillan GD, Lyle R, Ibberson M, De Palma M. Endogenous RNAs modulate microRNA sorting to exosomes and transfer to acceptor cells. Cell Rep. 2014; 8:1432–1446. [PubMed: 25159140]

Sung BH, Ketova T, Hoshino D, Zijlstra A, Weaver AM. Directional cell movement through tissues is controlled by exosome secretion. Nat Commun. 2015; 6:7164. [PubMed: 25968605]

Théry C, Amigorena S, Raposo G, Clayton A. Isolation and characterization of exosomes from cell culture supernatants and biological fluids. Curr Protoc Cell Biol. 2006; Chapter 3 Unit 3.22.

Turchinovich A, Weiz L, Langheinz A, Burwinkel B. Characterization of extracellular circulating microRNA. Nucleic Acids Res. 2011; 39:7223–7233. [PubMed: 21609964]

Valadi H, Ekström K, Bossios A, Sjöstrand M, Lee JJ, Lötvall JO. Exosome-mediated transfer of mRNAs and microRNAs is a novel mechanism of genetic exchange between cells. Nat Cell Biol. 2007; 9:654–659. [PubMed: 17486113]

Van Deun J, Mestdagh P, Sormunen R, Cocquyt V, Vermaelen K, Vandesompele J, Bracke M, De Wever O, Hendrix A. The impact of disparate isolation methods for extracellular vesicles on downstream RNA profiling. J Extracell Vesicles. 2014; 3 http://dx.doi.org/10.3402/jev.v3.24858.

Vickers KC, Palmisano BT, Shoucri BM, Shamburek RD, Remaley AT. MicroRNAs are transported in plasma and delivered to recipient cells by high-density lipoproteins. Nat Cell Biol. 2011; 13:423–433. [PubMed: 21423178]

Villarroya-Beltri C, Gutiérrez-Vázquez C, Sánchez-Cabo F, Pérez-Hernández D, Vázquez J, Martin-Cofreces N, Martinez-Herrera DJ, Pascual-Montano A, Mittelbrunn M, Sánchez-Madrid F. Sumoylated hnRNPA2B1 controls the sorting of miRNAs into exosomes through binding to specific motifs. Nat Commun. 2013; 4:2980. [PubMed: 24356509]

Zeng Y, Sankala H, Zhang X, Graves PR. Phosphorylation of Argonaute 2 at serine-387 facilitates its localization to processing bodies. Biochem J. 2008; 413:429–436. [PubMed: 18476811]

Highlights

- Active KRAS suppresses Ago2 interaction with endosomes and secretion into exosomes
- KRAS-MEK-ERK signaling promotes Ago2 phosphorylation on serine 387
- S387 phosphorylation inhibits Ago2-endosome association and sorting to exosomes
- Ago2 levels and phosphorylation control secretion of candidate miRNAs in exosomes

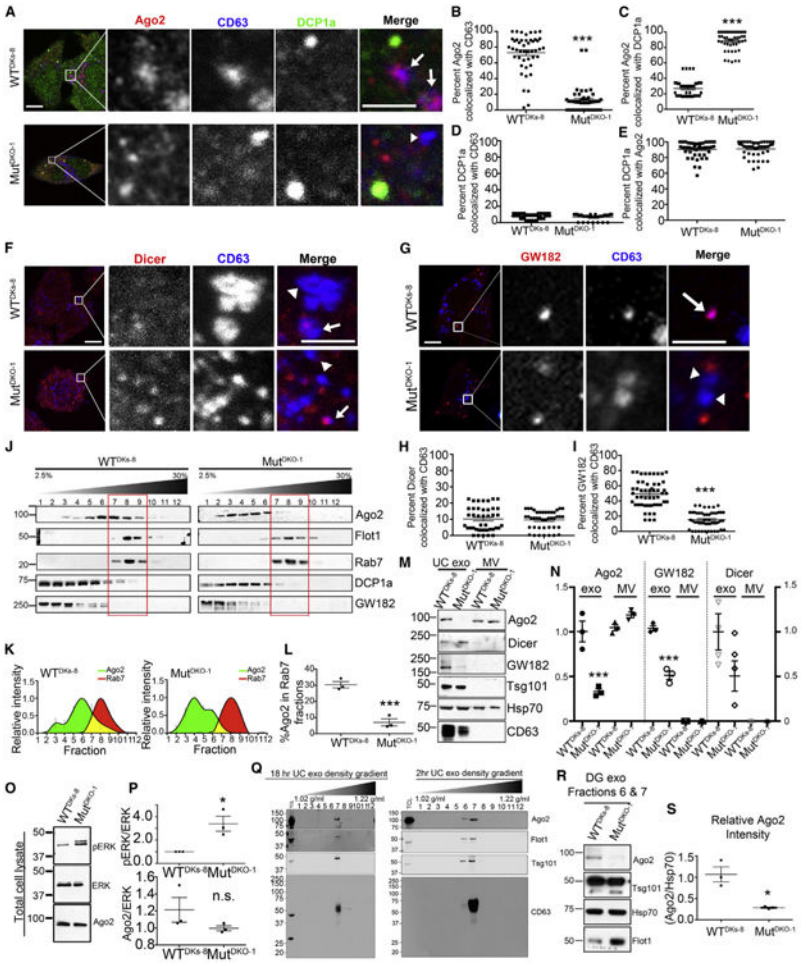

Figure 1. Mutant KRAS Regulates Ago2 Localization and Secretion

(A) Representative confocal immunofluorescence images of Ago2 (red), CD63 (blue), and DCP1a (green) in WT^{DKs-8} or Mut^{DKO-1} cells. Zooms from boxed areas are adjacent to the full images. Arrows point to Ago2-CD63 colocalization and arrowheads point to CD63-positive foci without Ago2. Scale bars represent 10 μm for full images and 5 μm for insets.

(B–E) Quantitation of colocalizations from images, as indicated. n ≥ 51 cells from three independent experiments for all.

(F and G) Confocal images of Dicer (F) or GW182 (G) (red) and CD63 (blue) in WT^{DKs-8} and Mut^{DKO-1} cells.

(H and I) Percent Dicer (H) or GW182 (I) colocalized with CD63 (n ≥ 50 cells from three independent experiments).

(J) Western blot analysis of Mut^{DKO-1} and WT^{DKs-8} subcellular fractionations through a continuous iodixanol gradient (2.5%–30%) for Ago2, MVE (Flotillin 1 and Rab7), and P-body components (DCP1a and GW182).

(K) Relative intensities of Ago2 (green) and Rab7 (red) bands for WT^{DKs-8} (left) and Mut^{DKO-1} (right) cell fractionations. Yellow represents overlapping fractions.

(L) Percentage of Ago2 in Rab7-positive fractions from three independent experiments.

(M and N) Representative western blots (M) and quantification (N) from three independent experiments analyzing equal numbers of MVs and UC exosomes (exo) from WT^{DKs-8} and Mut^{DKO-1} cells. Ago2, GW182, and Dicer bands normalized to Hsp70 as a loading control.
(O) Representative western blots of total cell lysates from WT^{DKs-8} and Mut^{DKO-1} cells.
(P) Quantification of Ago2 and pERK bands, normalized to total ERK from three independent experiments.
(Q) Western blot analysis of Ago2, Flotillin1 (Flot1), Tsg101, and CD63 from iodixanol density gradient (5%–40%) separation of 18-hr (left) and 2-hr (right) UC exosomes from WT^{DKs-8} cells.
(R) Fractions 6 and 7 from iodixanol density purification of 18-hr UC exosomes were pooled, and western blot analysis of equal numbers of exosomes was performed for Ago2, Hsp70, and Flotillin1.
(S) Quantification of Ago2 bands, normalized to Hsp70 from three independent experiments. Graphs depict mean ± SEM. *$p < 0.05$; ***$p < 0.001$; n.s., not significant. Uncropped blots and enlarged images are shown in Supplemental Appendices A and B for all figures.
See also Figure S1.

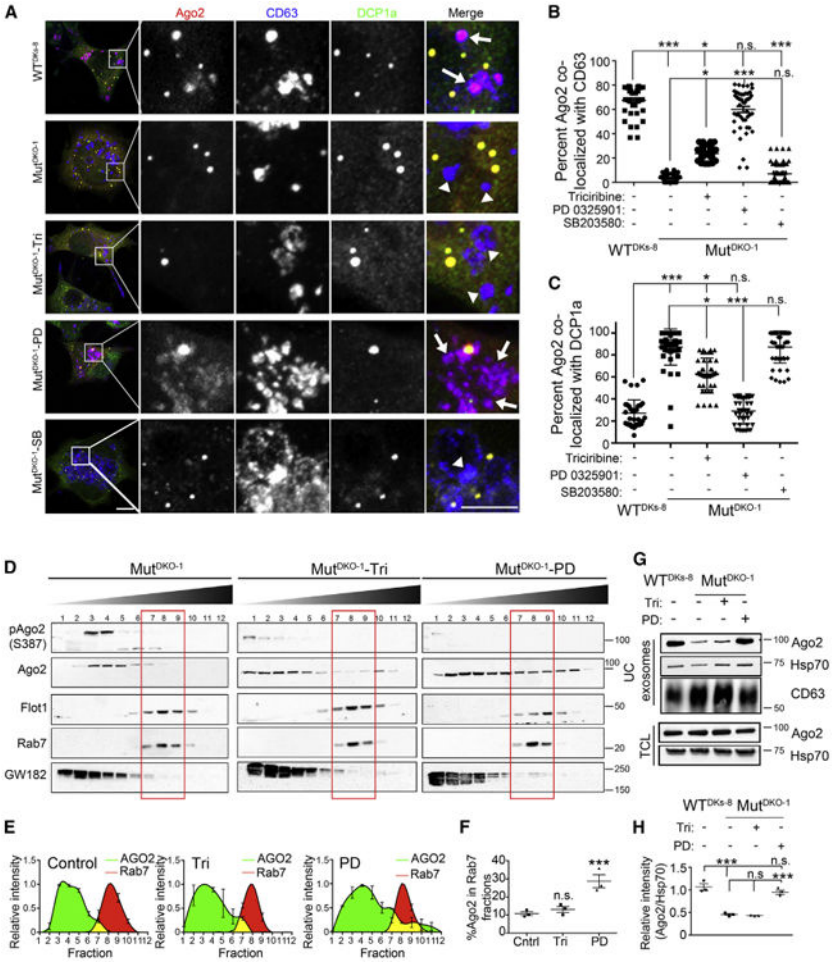

Figure 2. MEK and ERK Signaling Downstream of KRAS Regulates Subcellular Ago2 Localization and Secretion into Exosomes

(A) Representative confocal images of Ago2 (red), CD63 (blue), and DCP1a (green) in WT^{DKs-8}, Mut^{DKO-1},or Mut^{DKO-1} cells treated with 10 μM triciribine (Tri), 10 μM PD-0325901 (PD), or 20 μM SB203580 (SB) for 4 hr. Zooms of boxed areas are to the right of full images. Arrows point to Ago2-CD63 colocalization, and arrowheads point to CD63 positive foci without Ago2. Scale bars represent 10 μm (image) and 5 μm (zoom).

(B and C) Quantitation of colocalizations from images, as indicated ($n \geq 52$ cells from three independent experiments).

(D) Subcellular fractionation of Mut^{DKO-1} cells treated with 10 μM triciribine (DKO1-Tri) or 10 μM PD-0325901 (DKO1-PD).

(E) Relative intensities of Ago2 (green) and Rab7 (red) bands.

(F) Percent Ago2 present in Rab7-positive fractions from three independent experiments.

(G) Western blot analysis of equal numbers of exosomes and total cell lysates (TCL) from WT^{DKs-8} and Mut^{DKO-1} cells treated with the indicated compounds for 48 hr.

(H) Quantitation of Ago2 band levels for exosomes in western blots normalized to Hsp70 from four independent experiments.

Graphs depict mean ± SEM *p < 0.05; **p < 0.01; ***p < 0.001; n.s., not significant. For (A), brightness was uniformly increased after analysis in all channels for improved visualization.

See also Figure S2.

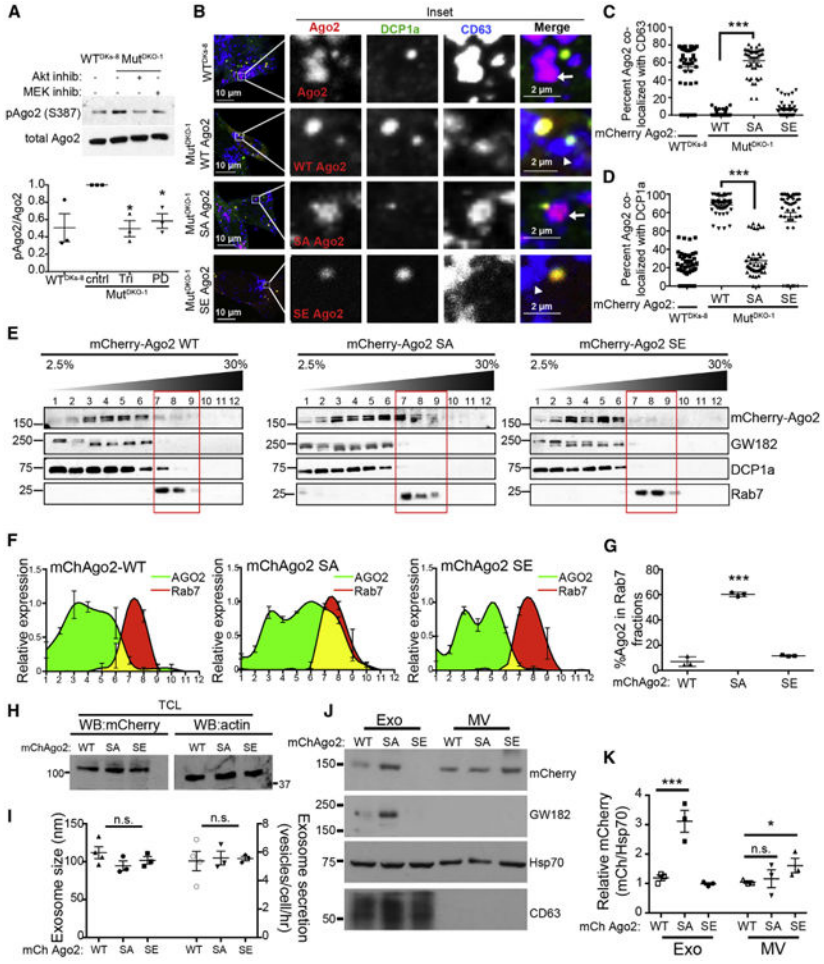

Figure 3. Phosphorylation of Ago2 at Ser387 Regulates Ago2 Trafficking and Secretion

(A) Western blot analysis of total cell lysates from WT^{DKs-8}, Mut^{DKO-1}, or Mut^{DKO-1} cells treated with 10 μM triciribine (Tri) or PD-0325901 (PD) (Akt and MEK inhibitors [inhib], respectively). Graph plots the ratio of pAgo2 to total Ago2 relative to that from Mut^{DKO-1} cells from three independent experiments. cntrl, control

(B–D) Immunofluorescent colocalization analysis of WT^{DKs-8} cells expressing mCherry-WT Ago2 (WT-Ago2) and Mut^{DKO-1} cells expressing either mCherry-WT, -S387A, or -S387E Ago2 mutants (red) costained for DCP1a (green) and CD63 (blue). (B) Representative confocal images. Zooms of boxed regions are to the right of the full images. Arrows point to Ago2-CD63 complexes, and arrowheads point to CD63-positive foci without Ago2. (C and D) Percent Ago2 colocalized with CD63 (C) or DCP1a (D), as indicated ($n \geq 50$ cells from three independent experiments).

(E–G) Subcellular fractionation analysis. (E) Representative western blots from density gradient subcellular fractionation of Mut^{DKO-1} cells expressing WT, S387E (SE), or S387A (SA) Ago2. (F) Relative intensities of Ago2 (green) and Rab7 (red) bands. (G) Percent Ago2 in Rab7-positive iodixanol fractions from three independent experiments.

(H) Representative western blot (WB) analysis of mCherry and actin levels in total cell lysates (TCL) from Mut^{DKO-1} cells expressing mCherry-WT, -S387E, or -S387A Ago2.

(I–K) NanoSight analysis (I) and western blot analysis (J and K, equal vesicle numbers loaded) of exosomes purified from mCherry-WT, -S387E, or -S387A Ago2 cells from three independent experiments.

Graphs depict mean ± SEM from three independent experiments. *$p < 0.05$; ***$p < 0.001$; n.s., not significant. For (B), brightness was uniformly increased after analysis in all channels for improved visualization.

See also Figure S3.

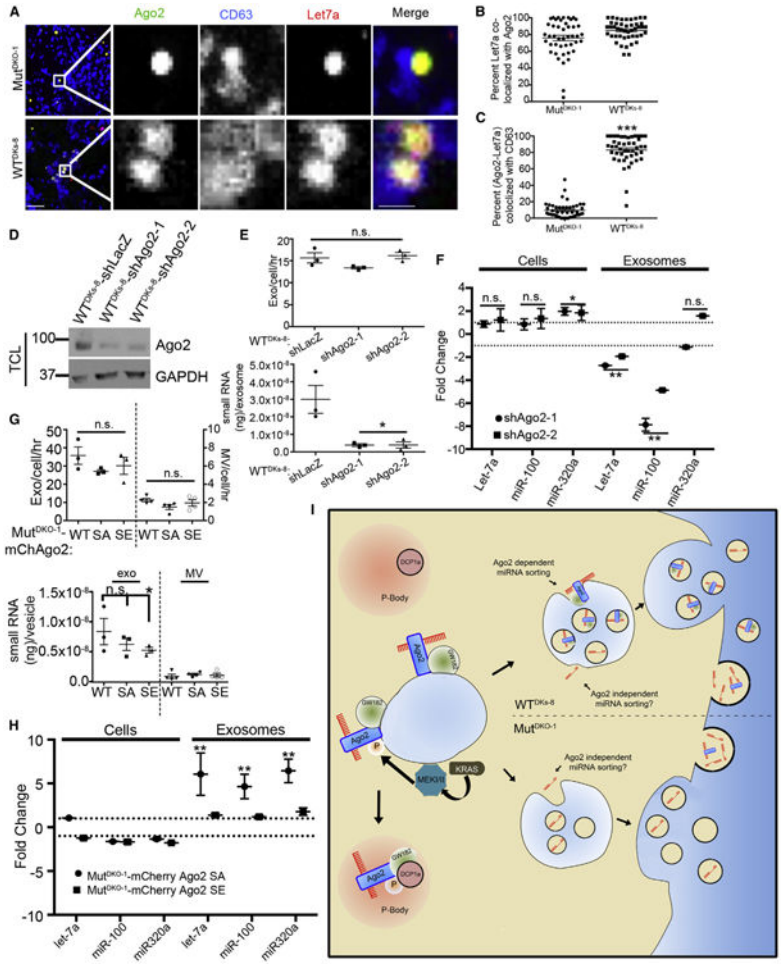

Figure 4. Ago2 Regulates miRNA Secretion into Exosomes

(A–C) Mut^{DKO-1} and WT^{DKs-8} cells expressing Cy3-labeled *let-7a* (red) were immunostained for CD63 (blue) and Ago2 (green). (A) Representative confocal images. Zooms of boxed areas are to the right of the full images. Scale bars represent 10 μm for full images and 2 μm for insets. (B) Percent *let-7a* colocalized with Ago2.

(C) Percent Ago2-*let-7a* complexes colocalized with CD63 (n ≥ 46 cells from three independent experiments).

(D) Western blot showing Ago2 expression in total cell lysates (TCL) from control or Ago2-KD cells.

(E) Exosome (Exo) secretion rate of control or Ago2-KD cells, quantitated by NanoSight analysis (upper graph), and the total amount of small RNAs present in those exosomes (lower graph).

(F) qRT-PCR of select miRNAs from exosomal and cellular RNA isolated from control and Ago2-KD cells. Graph shows fold change compared to shLacZ. Dotted lines indicate no fold change. WT, mCherry-WT; SE, mCherry-S387E; SA, mCherry-S387A.

(G) Exosome secretion rate of mCherry-Ago2-expressing Mut^{DKO-1} cell lines (upper graph) and the total amount of small RNAs present in those vesicles (lower graph).

(H) qRT-PCR of the indicated miRNAs from exosomal and cellular RNA. Data for Ago2-S387E or -S387A are represented as fold change compared to data for Ago2-WT. Dotted lines indicate no fold change.

(I) Model depicting Ago2-dependent and Ago2-independent sorting of miRNAs downstream of KRAS. In cells with minimal KRAS-MEK signaling (e.g., quiescent normal cells or carcinoma cells without KRAS mutations), Ago2-GW182-miRNA complexes are sorted into exosomes. By contrast,overly active KRAS stimulates MEK activity on MVE, leading to Ago2 phosphorylation and a shift from MVE to P-body association. This mechanism is likely to affect the sorting of Ago2-binding miRNAs to exosomes. Ago2-independent mechanisms are also likely to control trafficking of some miRNAs. As KRAS-MEK signaling does not affect the level of Ago2 in MVs, it is unlikely to affect the sorting of Ago2-binding miRNAs into shed MVs.

Graphs depict mean ± SEM from three independent experiments. *$p < 0.05$; **$p < 0.01$; ***$p < 0.001$; n.s., not significant.

See also Table S1.